Magneto-induced large deformation and high-damping performance of a magnetorheological plastomer

2014 Smart Mater. Struct. 23 105028

(http://iopscience.iop.org/0964-1726/23/10/105028)

IOP Publishing Smart Materials and Structures
Smart Mater. Struct. **23** (2014) 105028 (10pp) doi:10.1088/0964-1726/23/10/105028

Magneto-induced large deformation and high-damping performance of a magnetorheological plastomer

Taixiang Liu, Xinglong Gong, Yangguang Xu, Haoming Pang and Shouhu Xuan

CAS Key Laboratory of Mechanical Behavior and Design of Materials, Department of Modern Mechanics, University of Science and Technology of China, Hefei, 230027, People's Republic of China

E-mail: gongxl@ustc.edu.cn

Received 24 April 2014, revised 23 July 2014
Accepted for publication 6 August 2014
Published 16 September 2014

Abstract

A magnetorheological plastomer (MRP) is a new kind of soft magneto-sensitive polymeric composite. This work reports on the large magneto-deforming effect and high magneto-damping performance of MRPs under a quasi-statical shearing condition. We demonstrate that an MRP possesses a magnetically sensitive malleability, and its magneto-mechanical behavior can be analytically described by the magneto-enhanced Bingham fluid-like model. The magneto-induced axial stress, which drives the deformation of the MRP with 70 wt % carbonyl iron powder, can be tuned in a large range from nearly 0.0 kPa to 55.4 kPa by an external 662.6 kA m^{-1} magnetic field. The damping performance of an MRP has a significant correlation with the magnetic strength, shear rate, carbonyl iron content and shear strain amplitude. For an MRP with 60 wt % carbonyl iron powder, the relative magneto-enhanced damping effect can reach as high as 716.2% under a quasi-statically shearing condition. Furthermore, the related physical mechanism is proposed, and we reveal that the magneto-induced, particle-assembled microstructure directs the magneto-mechanical behavior of the MRP.

Keywords: magnetorheological plastomer, magneto-damping effect, magneto-mechanical behavior

(Some figures may appear in colour only in the online journal)

1. Introduction

A magnetorheological plastomer (MRP) is a new kind of soft magneto-sensitive polymeric composite material, which has a novel performance in magnetorheology [1]. In the usual way, an MRP is prepared by dispersing micron-sized magnetic or magnetizable particles into magnetically insensitive, soft polymer matrixes. An MRP behaves as an intermediate state between traditional fluid-like magnetorheological fluid (MRF) [2–6] and conventional solid-like magnetorheological elastomers (MREs) [7–9]. In contrast to the easily sedimentary MRF and the relatively low- magnetorheological-effect MRE, an MRP attractively possesses long-time stability and a higher magnetorheological effect. Under usual conditions, the internal magnetizable particles in an MRP cannot move by themselves due to the constraint of the matrix. However, when an external magnetic field is applied to an MRP, the internal particles will overcome the constraint of the matrix and can rearrange into some ordered microstructures. The ordered microstructures will be kept in the MRP while the external magnetic field is switched off or removed. Correspondingly, it is worth noting that the microstructure-based physical properties (e.g. the electric conductivity, thermal conductivity, acoustic conductivity, etc) of the MRP change significantly once the external field is removed. These conducting properties are vital in practical sensors and actuators. With its novel performance in magnetorheology, MRPs are very promising for use as a new or alternative material in many practical applications, such as magneto-dampers [10–12], energy absorbers [13, 14] and vibration isolators

[15, 16], especially in magneto-sensitive sensors and actuators [17–19], etc.

A typical soft polyurethane-based MRP composited with carbonyl iron powder was prepared and reported in our group's previous work [1]. It was shown that the chain-like microstructure was formed when an external magnetic field was applied to an MRP, and the microstructure was kept in the MRP after switching off the external magnetic field. Conventional magnetic sweep tests were implemented to study the dynamic properties of the MRP and showed that the magneto-induced storage modulus and the relative magnetorheological effect of the MRP with 80% carbonyl iron powder could respectively reach as high as 6.54 MPa and 532% under an external 662.6 kA m^{-1} magnetic field. In addition, the static time-dependent creep and recovery behaviors of the MRP and the dynamic behavior of the MRP under oscillatory shear rheometry were systematically investigated [20, 21] and provided a certain reference to the design and development of applicatory devices for static and dynamic cases, respectively. However, it is still necessary to point out that many practical damping or actuating apparatuses work in the case of large deformation and quasi-static shear such as in bridge engineering, high-rise building engineering, vehicle system control, etc. The quasi-static loading rate is neither a static rate nor a dynamic rate, but it serves as a bridge between the static and dynamic loading rates. The magneto-damping performance of apparatuses partly depends on the magneto-deforming capacity of the useable material. For these apparatuses, the material with the larger magneto-deforming capacity and higher magneto-damping performance is much needed. The magneto-mechanical behavior of the useable material has a great effect on the performance of the apparatuses; therefore, for the high-performance MRP, it is imperative to study its magneto-deforming effect and magneto-damping performance under cyclically and quasi-statically shearing conditions and to understand the relative physical mechanism.

This work focuses on the magneto-induced large deformation effect of MRPs and the magneto-damping performance of MRPs under cyclically and quasi-statically shearing conditions. Firstly, a sample of magneto-induced large deformation is intuitively given, and the related magneto-induced stress in the MRP is discussed. Then, the magneto-damping performance of the MRP under a cyclically and quasi-statically shearing condition with different samples, shear rates and strain amplitudes in the absence/presence of an external magnetic field are investigated. Correspondingly, the microstructure-based physical mechanisms of these behaviors are further discussed according to the relative experimental results.

2. Experimental

To prepare the MRP sample, a visco-flowing plastic matrix must first be synthesized. The matrix can be synthesized from toluene diisocyanate (TDI, 2,4-TDI at ~80%, 2,6-TDI at ~20%, Tokyo Chemical Industry Co. Ltd, Japan) and polypropylene glycol (PPG-1000, Sigma-Aldrich Trading Co. Ltd, Shanghai, China) with the ratio 3:1. We mixed the raw materials into a three-necked round-bottom flask at 75 °C and then stirred the mixture for 2 h. Subsequently, we lowered the temperature of the mixture to 65 °C and dropwise added a small quantity of stannous octoate and a moderate amount of acetone (both provided by Sinopharm Chemical Reagent Co. Ltd, China) into the flask to accelerate the cross-linking reaction and avoid gelating. Twenty minutes later, the synthesis process of the matrix was finished. Once the matrix was synthesized, we immediately added a soft magnetic powder into the matrix and adequately blended the mixture before cooling the matrix down; thus, the MRP sample was prepared.

In our experiment, we added soft-magnetic carbonyl iron powder (CIP, type CN, 7.200 g · cm^{-3} in true density, produced by BASF aktiengesellschaft, Germany) into the prepared plastic polyurethane matrix (0.986 g · cm^{-3} in density) with the CIP's weight ratio of 40%, 50%, 60% and 70% in the mixture to the volume fraction of 8.4%, 12.0%, 17.0%, and 24.2% of the carbonyl iron powder, respectively, in the mixture. Correspondingly, we denote these samples as MRP-40, MRP-50, MRP-60 and MRP-70, respectively.

3. Magneto-induced large deformation of an MRP

For a magneto-sensitive and shape-changeable MRP, it is interesting to explore the shape-changing process of an MRP with different initial shapes and/or under a different magnetic field. If the exterior shape-change of the material is of prime interest, Digital Image Correlation (DIC) and interferometry techniques provide the user with mature experimental approaches that may meet the demand [22]. It is also commonly known that a basic mechanical behavior always drives the deformation of the material. However, it is difficult or impossible to simultaneously measure the deformation of the material and the relative mechanical behavior. Recently, magneto-induced normal (or axial) force/stress in an MRF [23, 24] and in magnetorheological gel [25–27] under axially constrained and/or slow loading conditions were well studied, providing us with useful references.

To explore the magneto-induced large deformation of an MRP, we chose MRP-70 as a test sample and used a commercial magnetic field generator (S&T Tech. Inc., Beijing, China) to generate the desired magnetic field. As shown in figure 1(a), we firstly shaped the MRP-70 into a small sphere and put it into the magnetic field generator; then, we quickly switched on a 585 kA m^{-1} magnetic field (i.e. about 735 mT in magnetic intensity). Thirty seconds later, the initiated sphere shape changed into a shuttle-like shape (figure 1(b)). Meanwhile, the shuttle-shaped MRP-70 connected the upper and lower magnetic poles into a magnetic conducting channel. When the current of the upper magnetic pole would be switched off, the shuttle-shaped MRP-70 would shrink back to the lower pole. This delaying connecting and shrinking effect makes MRPs promising for switches in situations in which avoiding destructive impact is needed. We shaped the

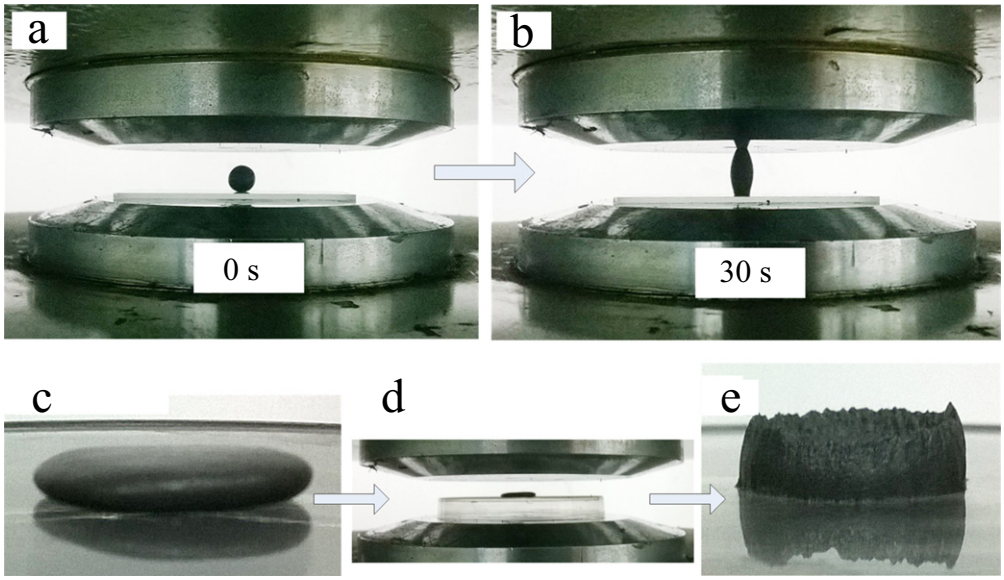

Figure 1. The large deformation of the magneto-sensitive MRP-70 under a uniform 585 kAm^{-1} magnetic field. In the upper series, the small sphere-shaped MRP-70 at an initial 0 s (a) changes its shape into a shuttle-like shape at 30 s (b). In the lower series, the initial oblate shape of MRP-70 (c) is changed into a parallel column-like shape (e) by the external magnetic field.

MRP-70 into an oblate shape (figure 1(c)) and placed it into the magnetic field generator (figure 1(d)); it was apparent that the MRP-70 gradually swelled considerably along the direction of the magnetic field (figure 1(e)) after a 585 kA m^{-1} magnetic field was switched on. For an incompressible material, the MRP's volume barely changes when the external magnetic strength is varied. However, the internal particle-assembled microstructure is magnetically field-dependent. This dependence causes the morphology of the MRP to change along with the external magnetic field, and it contributes to the directional swell. The swelling effect makes the MRP applicable as a force actuator in vibration control or others, not only for slow or delay actuating but also for quick actuating. This will be discussed below.

To study the magneto-induced stress of an MRP, we used a commercial rheometer Physica MCR301 (produced by Anton Paar GmbH, Austria) equipped with an electromagnetic accessory MRD180 to do the test. The sketch of the test system is shown in the inset of figure 2. The MRP sample is placed between an electromagnet substratum and an upper rotatable non-magnetism plate (i.e. the rotor). Here, we define the vertical direction perpendicular to the substratum as the normal direction. The magnetizer cover is used to strengthen the magnetic field and make it uniform in the area in which the sample is placed. The following experiments were all conducted at room temperature 25 °C.

The magneto-induced normal stress σ_n of the MRP that evolved with the slow-loading external magnetic field is shown in figure 2. In the tests, the strength of the magnetic field increases linearly from an initial 0.0 kA m^{-1} to a final 293.0 kA $\cdot$ m^{-1} in 60 min. However, the magneto-normal stress does not increase linearly along with the increasing magnetic strength. When the magnetic strength is smaller than 50.0 kA m^{-1} (as the dash-dot arrow indicates in figure 2), the magneto-normal stress barely changes with the increasing the

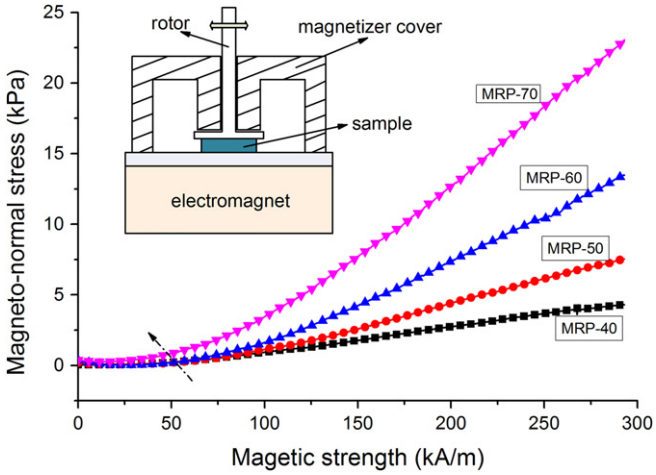

Figure 2. Magneto-induced normal stress σ_n of the MRP that evolves with the slow loading of the external magnetic field. The inset is the sketch of the Physica MCR301 test system.

magnetic strength. The magneto-normal stress linearly increases along with the increasing magnetic strength when the magnetic strength is greater than 50.0 kA m^{-1}. When an external 662.6 kA m^{-1} magnetic field is suddenly applied, the magneto-stress gets a sudden increment in the beginning and then gradually plateaus (as figure 3 shows) with time. The microstructural evolution that relates to the evolving magneto-induced normal stress has been studied in our previous work [28, 29]. As shown in the inset of figure 3, the internal particle-formed microstructure evolves from initial random dispersion (figure 3(a)) to an unstable chain-like structure (figure 3(b)) and then to a stable column-like structure (figure 3(c)). The macroscopic magneto-induced normal stress results from interparticle attraction and extrusion along the magnetic field's direction, and the magnitude of the stress can reach as high as 55.4 kPa. Moreover, one can clearly

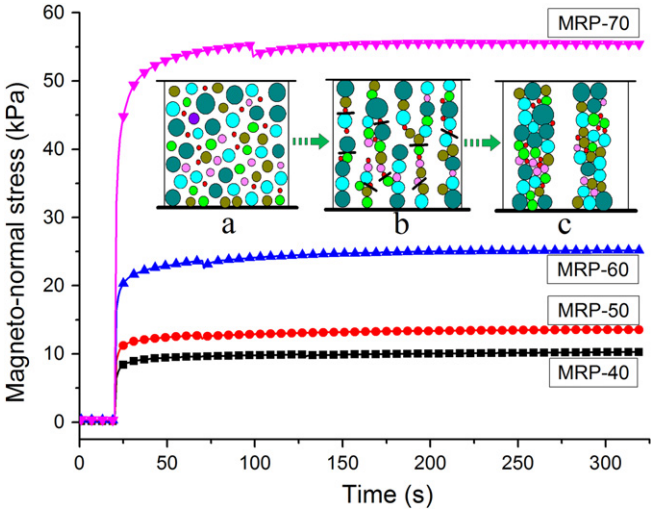

Figure 3. Magneto-induced normal stress σ_n of the MRP that evolves with the transient loading of the external 662.6 kAm^{-1} magnetic field. The insets show the internal microstructure of the MRP, which progresses from initial random dispersion (a) to an unstable chain-like configuration (b) and then to a stable column-like pattern (c).

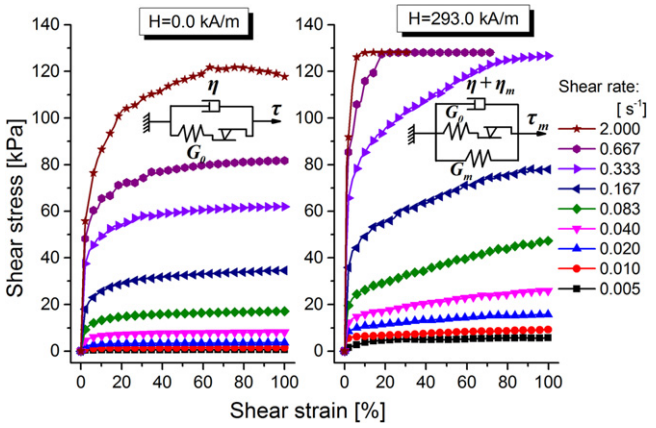

Figure 4. The shear stress-strain curves of the MRP-60 with (right) and without (left) an external magnetic field under different shearing-rate conditions. Respectively, the inset shows the MRP's analytical models in the absence and presence of an external magnetic field.

determine that the carbonyl iron content in an MRP can greatly affect the magneto-induced stress. From the above two tests, one can see that the MRP has great potential for use in a force actuator for either slow or quick actuating.

4. Magneto-damping performance of an MRP under a quasi-statically shearing condition

In practice, damping materials usually work in the quasi-static shearing mode for vibration control or for anti-seismic applications such as in bridge engineering, high-rise building engineering, vehicle system control, etc. As a recently reported smart magnetorheological material, a high-performance MRP shows attractive potential for the above-mentioned practical applications. However, the mechanical behaviors of an MRP under cyclically and quasi-statically shearing conditions have not been studied until now. Given this information, the following work will focus on the MRP's mechanical behavior under a quasi-statically shearing condition with different CIP contents, shearing rates and strain amplitudes in the absence/presence of external magnetic strength. The tests were conducted with a Physica MCR301 rheometer, and the temperature in each test was stably controlled at 25 °C.

4.1. Mechanical behavior under a simple shearing condition

Considering that the MRP prospectively works in a quasi-static shearing mode, the basic rate-dependent shear stress-strain curve of the MRP is tested and discussed. For example, the shear stress-strain curves of the MRP-60 under different shearing-rate conditions with/without an external magnetic field are presented in figure 4. In the test, the shear strain progresses linearly from an initial 0% to 100% in the different times of 0.5 s, 1.5 s, 3.0 s, 6.0 s, 12.0 s, 25.0 s, 50.0 s, 100.0 s and 200.0 s, respectively. The corresponding shear rates in the test are labeled in the right side of figure 4.

In the absence of an external magnetic field (i.e. the external magnetic strength H = 0.0 kA m^{-1}), the shear stress τ gets a sudden increment at the beginning and then plateaus in a short time with the enlargement of the shear strain. This mechanical behavior can be described using the conventional viscoelastic-plastic Bingham fluid-like model:

$$\tau = \begin{cases} G_0\gamma + \eta\dot{\gamma}, & \text{for} \quad \gamma < \gamma_0 \\ G_0\gamma_0 + \eta\dot{\gamma}, & \text{for} \quad \gamma \geqslant \gamma_0 \end{cases} \tag{1}$$

in which, τ is the shear stress, G_0 is the initial shear modulus, γ is the shear strain, γ_0 is the yield shear strain, η is the equivalent flowing viscosity and $\dot{\gamma}$ is the shear rate. The equivalent analytical model of this mechanical behavior is shown as the inset of figure 4 (in 'H = 0.0 kA m^{-1}'), which is constructed by a dashpot that is parallel to a cascade of a spring and a slider. γ_0 and G_0 reflect the MRP's initial elasticity, including the elasticity of the polyurethane matrix, the elasticity of the carbonyl iron particle and the elastic interaction between the matrix and the particle. After the yield, the mechanical behavior of the MRP can be characterized by η, which depends on the flow of the matrix itself and the relative slip between the matrix and the particle. From the experimental results, the values of γ_0, G_0, and η in the analytic model can be estimated in the order of 5.0%, 15.0 kPa and 107.8 kPa · s (when the shear rate is $\dot{\gamma} = 0.083$ s^{-1}), respectively, which indicates that the MRP-60 is a high-viscosity material with a certain low-yield strength. One can determine that the MRP-60 possesses good plastic malleability and behaves in a highly rate-dependent manner.

In the presence of an external magnetic field (i.e. H = 293.0 kA m^{-1}), the mechanical shear stress-strain behavior of the MRP-60 under different shearing conditions can be seen from the right subfigure of figure 4. Before the test, a 662.6 kA m^{-1} magnetic field is applied and kept for 300 s to

adequately preconfigure the internal particle-formed microstructure in the MRP-60. One can see that the shear stress also gets a sudden increment at the beginning of the shear strain's progress; however, the shear stress then linearly and continuously increases with the increasing shear strain. This progress of the shear stress-strain behavior greatly differs to that in the absence of an external magnetic field. Here, it can clearly be seen that a plateau occurs when the shear rate is larger than 0.333 s^{-1}; this is because the shear stress, which is needed to overcome the yield stress and drive the flow of the MRP-60, exceeds the friction stress between the test plate and the sample. That is to say, slipping occurs at the contact interface between the test plate and the sample. Given this information, the following discussion will only focus on the test results when the shear rate is less than or equal to 0.333 s^{-1}. To describe the mechanical behavior of the MRP under an external magnetic field, a modified Bingham fluid-like model is proposed as:

$$\tau_m = \begin{cases} G_0\gamma + G_m\gamma + (\eta_m + \eta)\dot{\gamma}, \ for\ \gamma < \gamma_0 \\ G_0\gamma_0 + G_m\gamma + (\eta_m + \eta)\dot{\gamma}, \ for\ \gamma \geqslant \gamma_0 \end{cases}. \quad (2)$$

Here, τ_m is the shear stress in the presence of the external magnetic field, G_m is the magneto-induced shear modulus and η_m is the magneto-induced viscosity. The equivalent analytical model of this mechanical behavior can be recognized as a parallel combination of three elements: a magnetic relevant dashpot, a magnetic dependent spring and a spring-slider. G_m results from the interparticle magnetic interaction, which depends on the strength of the external magnetic field and the internal particle-assembled microstructure of the MRP. The interparticle magnetic interaction resists the shear deformation of the MRP and persistently contributes to the strength of the shear modulus. Similarly, the interparticle magnetic interaction resists the flow of the MRP in the post-yield range and enhances the effective viscosity of the MRP, introducing a magneto-induced increment of viscosity η_m. According to the experimental results, the value of G_m and η_m can be estimated on the order of 20.2 kPa and 119.4 kPa · s (when the shear rate is $\dot{\gamma}$ = 0.083 s^{-1}), respectively. Considering the initial shear modulus G_0 = 15.0 kPa) and the viscosity η = 107.8 kPa · s of the MRP-60 under no external magnetic field, one can determine that the external magnetic field can substantially affect the property of an MRP. Similar works on the modeling of the field-induced plasticity and magneto-dipolar striction of soft magnetic elastomers were well done [30–32].

4.2. Mechanical behavior under a cyclically shearing condition without an external magnetic field

In a low-frenquency damper, the damping material usually works under a cyclically shearing condition in a passive mode without an external magnetic field. The performances of a damper, such as the strength of the resistance and the capacity of the energy absorption, directly depend on the mechanical behavior of the damping material. Thus, for the prospective damping material of the MRP, it is imperative to study the basic mechanical behavior of the MRP under a cyclically and quasi-statically shearing condition. In the following work, we will firstly study the effect of CIP content in an MRP; then, the effect of the shear rate and the effect of the strain amplitude on a certain MRP sample, respectively, will be discussed. The following comparative tests are at the core of the MRP-60, with a shear rate of $\dot{\gamma}$ = 0.040 s^{-1} and a shear strain amplitude of A_0 = 100%; we mark this test as (MRP-60, $\dot{\gamma}$ = 0.040 s^{-1}, A_0 = 100%).

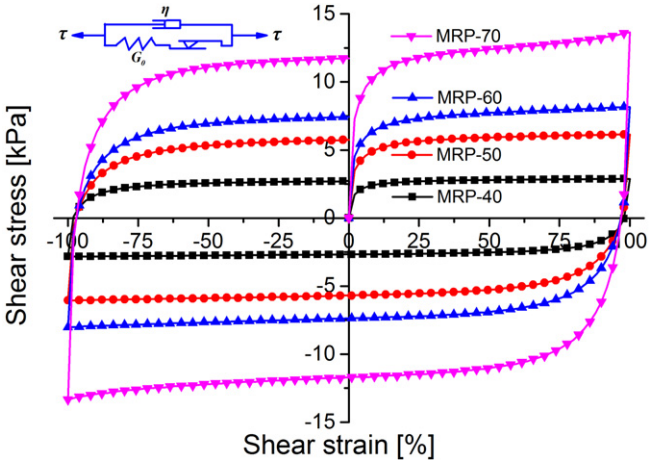

Figure 5. The shear stress-strain curves of different MRP samples under constant shear rate $|\dot{\gamma}|$ = 0.040 s^{-1} and strain amplitude A_0 = 100% without an external magnetic field. The top-left inset shows the analytical model of the MRP.

The effect of the CIP content on the mechanical behavior can be seen in figure 5. In all of the tests, the magnitude of shear rate $\dot{\gamma}$ is set as a constant of 0.040 s^{-1}, and shear strain amplitude A_0 is set as 100%. The shear strain progresses linearly from an initial 0% to 100% with the shear rate of $\dot{\gamma}$ = 0.040 s^{-1}; then, it immediately shifts back from 100% and inversely appoaches −100% with a constant shear rate of −0.040 s^{-1}. Then, the shear strain gruadually returns to 0% again from −100% with the shear rate 0.040 s^{-1}. Correspondingly, the shear stress gets a sudden increment at the beginning and then approaches a stable value at about γ = 25%. After the shear strain gets the maximum (inverse maximum) γ = 100% (−100%), the shear stress will inversely get a abrupt drop (rise); then, it becomes stable at about γ = 50%. The shear stress-strain curve draws a gapped hysteresis loop (directly referred to as 'loop' in the following context). The analytical model of this mechanical behavior can be discribed as the inset of figure 5. In figure 5, the area between the shear stress-strain curve and the horizontal axis denotes the density of the energy that is absorbed by the MRP during a cyclical process of shear strain. The larger the area, the more the energy absorption, and the stronger the MRP's damping. From figure 5, we can quantitively compare the sizes of the areas of MRP-40, MRP-50, MRP-60 and MRP-70 using the following integration:

$$\rho_E = \oint \tau d\gamma = \int_0^{A_0} \tau d\gamma + \int_{A_0}^{-A_0} \tau d\gamma + \int_{-A_0}^{0} \tau d\gamma. \quad (3)$$

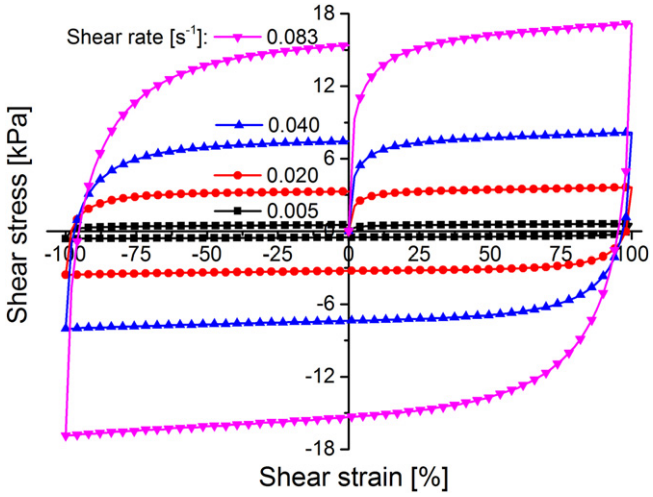

Figure 6. The shear stress-strain curve of the MRP-60 under a different shear rate and constant strain amplitude $A_0 = 100\%$ without an external magnetic field.

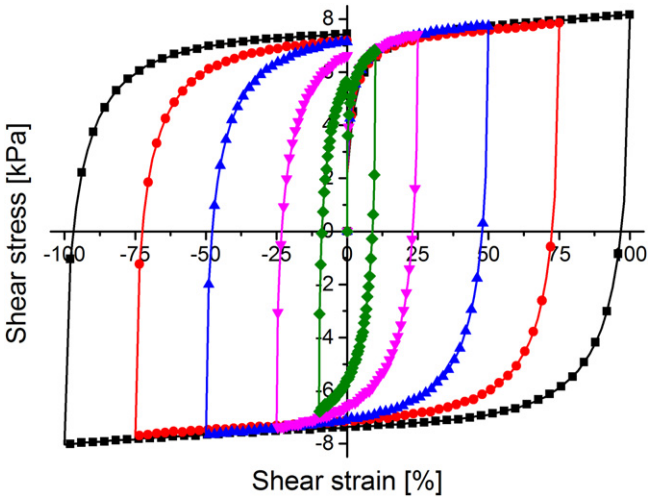

Figure 7. The shear stress-strain curve of the MRP-60 under a different strain amplitude and a constant shear rate $|\dot{\gamma}| = 0.040\ s^{-1}$ without an external magnetic field.

Here, A_0 is the shear strain amplitude 100%, τ is the shear stress in the absence of an external magnetic field, γ is the shear strain, and correspondingly the sizes of the areas or the density of the absorbed energy $\rho_E = 10.23$, 21.34, 27.82 and 44.71 $kJ \cdot m^{-3}$, respectively. Thus, one can determine that the greater the CIP content, the stronger the MRP's damping. With subjective understanding, we think that the addition of the CIP into the polyurethane matrix introduces the internal friction between the CIP and the matrix as well as the inter-particle friction of the CIP. As theCIP content increases, the effect of the internal friction gets stronger and stronger, which contributes to the damping of the MRP.

To study the shear rate's effect on the mechanical behavior of MRP, MRP-60 is chosen as a test sample, and the shear strain amplitude is set as a constant of 100%. The mechanical bahavior of the MRP-60 under different shearing-rate conditions without an external magnetic field can be found in figure 6. In each test, the shear strain progresses linearly from an initial 0% to 100%, and the shape of the shear stress-strain loop is very similar to the test (MRP-60, $\dot{\gamma} = 0.040\ s^{-1}$, $A_0 = 100\%$). One can clearly recognize that the larger the shear rate, the larger the area of the shear stress-strain loop. Corresponding to the shear stress-strain loops of the shear rates $\dot{\gamma} = 0.083$, 0.040, 0.020 and $0.005\ s^{-1}$, the sizes of the areas of the loops are 56.40, 27.82, 12.56 and 1.97 $kJ \cdot m^{-3}$, respectively. It is again shown that the MRP is a highly rate-dependent damping material. In other words, the larger the shear rate, the more the energy absorption and the higher the damping performance. Therefore, the rate-dependent mechanical behavior of the MRP must be take into account for the design of dampers in which the MRP can be prospectively used.

The effect of the shear strain amplitude on the MRP's mechanical behavior can be intuitively known from figure 7; the larger the shear-strain amplitude, the higher the damping performance. In the test, the magnitude of the shear rate is set as a constant of $0.040\ s^{-1}$. The shear stress-strain curves of the MRP-60 under different shear-strain amplitudes without an external magnetic field can be seen in figure 7. The effect of different shear strain amplitudes of 10%, 25%, 50%, 75% and 100% are comparatively studied. When the shear strain amplitude is small, e.g. 10% (the green-rhombus one in figure 7), the shear stress changes sharply with the shear strain, drawing a sharp hysteresis loop. When the shear strain amplitude is larger than 25%, the shear stress-strain loop gets increasingly stouter with the increasing shear strain amplitude, while the maximum shear stress hardly changes. In other words, the MRP mainly gets a plastic flow when the shear strain is larger than 25%. Corresponding to the shear strain amplitudes of 10%, 25%, 50%, 75% and 100%, the sizes of the loops' areas are 1.98, 5.86, 12.96, 19.98 and 27.83 $kJ \cdot m^{-3}$, respectively. The size of the loop area proportionally enlarges with the increasing shear strain amplitude, indicating that the damping performance of the MRP proportionally increases with the increasing shear strain amplitude. Usually, the larger the shear strain amplitude, the higher the MRP's damping performance; however, the magnitude of the shear strain amplitude is usually restricted by the size of the damper's external structure.

4.3. Mechanical behavior under a cyclically shearing condition with an external magnetic field

From the previous subsection, one can determine that the MRP is a prospective damping material for passive dampers. But for all of this, active controlling or actuating is usually needed and is necessary in many practical applications. As a magneto-sensitive material, an MRP has great potential for use in an active damper or actuator. To study the mechanical behavior of an MRP under a cyclically and quasi-statically shearing condition with an external magnetic field, the MRP-60 is also chosen as the test sample; then, the effect of the external magnetic strength and shear rate are discussed. Before the test, a 662.6 $kA\ m^{-1}$ magnetic field is applied and kept for 300 s to adequately configure the internal particle-

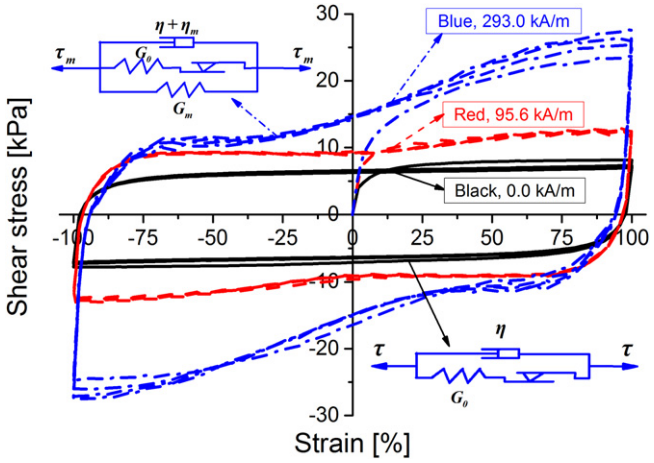

Figure 8. The shear stress-strain loops of the MRP-60 under a different external magnetic field with a constant magnitude of shear rate $|\dot{\gamma}| = 0.040\ s^{-1}$ and a shear strain amplitude $A_0 = 100\%$. The inset shows the analytical model of the MRP-60 under an external magnetic field.

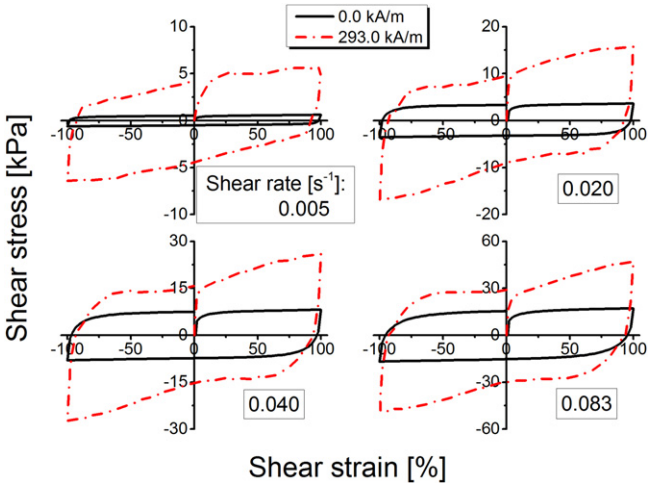

Figure 9. The mechanical behavior of the MRP-60 under a different shearing condition with or without an external 293.0 kAm^{-1} magnetic field.

assembled microstructure in the MRP-60. The varying process of the magneto-induced normal stress is compared to the cyclically shearing process under an external magnetic field and is discussed.

The shear stress-strain curve of the MRP-60 under a different external magnetic field can be found in figure 8. In each test, the shear strain continuously and repeatedly progresses four cycles with the constant magnitude of shear rate $|\dot{\gamma}| = 0.040\ s^{-1}$ and the shear-strain amplitude $A_0 = 100\%$. In the absence of an external magnetic field (i.e. $H = 0.0\ kA\ m^{-1}$, as the black curve in figure 8 shows), the shear stress-strain loops are oblate and well repeated. This mechanical behavior can be described via the analytical model in the bottom right in figure 8. By comparing the analytical model in figure 8 to the MRP model in figure 5, it is also found that the preconfigured MRP would behave similarly to the initial MRP with a randomly dispersed carbonyl iron powder after the external magnetic field is switched off since the microstructure that remained after the field was removed would quickly be disrupted upon shear or squeeze. The shear stress-strain relationship under an external 95.6 $kA\ m^{-1}$ magnetic field is shown as the red curve. From figure 2, one can determine that the 95.6 $kA\ m^{-1}$ magnetic field can only drive a very slow evolution of the microstructure in the MRP. That is to say, the evolution of the internal microstructure of the MRP is mainly affected by shear strain. The external magnetic field slightly affects the strength of the interparticle magnetic interaction and mainly contributes to the initial elasticity of the MRP. In the post-yield range, the magneto-induced interparticle interaction is not strong enough to resist the microstructural evolution induced by the shear deformation. Thus, the 'Red, 95.0 $kA\ m^{-1}$,' curve increases its height and keeps its shape quite similar to that of the 'Black, 0.0 $kA\ m^{-1}$,' curve. Under an external 293.0 $kA\ m^{-1}$ magnetic field (the strength is enough to drive a quick variation of the internal microstructure of the MRP), the mechanical behavior of the MRP-60 is shown as the 'Blue, 293.0 $kA\ m^{-1}$,' curve. In this curve, the shear stress sharply increases with the increasing the shear strain from the initial 0% and then progresses to the maximum stress in a fluctuating way. In the meantime, the configuration of the internal particle-formed microstructure changes greatly along with the shear stress's increasing size and wavelike progression. After the shear strain gets to the maximum and begins to inversely approach 0%, the shear stress abruptly drops and undergoes a fluctuating process in the subsequent ten seconds; then, it gradually approaches the inverse maximum. In the fluctuating process of the shear stress, the internal microstructure undergoes a very complex changing process, which includes the chain-like microstructure's complex rupture and reconstruction. Moreover, it is noticeable that the maximum of the shear stress can be enhanced after several shearing cycles. To the best of our knowledge, the cyclic shearing load induces a tighter microstructure along the direction of the external magnetic field, which contributes to the maximum shear stress. The macroscopic analytical model of this mechanical behavior can be qualitatively described in the top-left inset. Corresponding to the black, red and blue curves, the areas of the three colored loops are 24.24, 39.87 and 66.82 $kJ \cdot m^{-3}$, respectively, which indicates that the external magnetic field has a strong influence on the damping performance of the MRP.

In contrast to the mechanical behavior of the MRP-60 under no external magnetic field, the shear rate dependent mechanical behavior of the MRP-60 under a 293.0 $kA\ m^{-1}$ magnetic field is shown in figure 9. In the absence of an external magnetic field, the mechanical behavior of the MRP-60 can be described using equation (1); the areas of the shear stress-strain loops 0.005, 0.020, 0.040 and 0.083 s^{-1} (indicated by the solid black lines in figure 9) are 1.97, 12.56, 27.82 and 56.40 $kJ \cdot m^{-3}$, respectively. Under the 293.0 $kA\ m^{-1}$ magnetic field, the mechanical behavior can be qualitatively described using equation (2); the areas of the shear stress-strain loops are 16.08, 40.48, 67.30 and 124.17 $kJ \cdot m^{-3}$, respectively. Correspondingly, the relative magneto-induced enhancing effects are 716.2%, 222.3%,

141.9% and 120.2%, respectively. The relative magneto-induced enhancing effect is defined as the ratio of the area difference between the red dot-dash loop and the black solid loop to the area of the black solid loop. For example, in the top-right subfigure of figure 9, the area of the black solid loop is firstly calculated ($12.56\,\mathrm{kJ\cdot m^{-3}}$); then, the area of the red dot-dash loop ($40.48\,\mathrm{kJ\cdot m^{-3}}$) is calculated. Thus, the defined relative magneto-induced enhancing effect is calculated as $(40.48\text{-}12.56)/12.56\times 100\% \approx 222.3\%$. This value indicates how much the damping of the MRP is enhanced by the applied field. One can see that the relative magneto-induced enhancement decreases with the increasing shear rate, though the damping itself is greatly enhanced. In the case of a low shear rate condition (e.g. $\dot{\gamma} = 0.005\,\mathrm{s^{-1}}$), the external magnetic field has relatively enough time (e.g. 200 s) to drive the microstructural evolution, resulting in the macroscopic mechanical behavior that mainly depends on the magneto-induced microstructure and its evolution. In other words, the enhancement of the shear stress mainly results from the magneto-induced enhancement of the initial shear yield stress. In the case of a high shear rate condition (e.g. $\dot{\gamma} = 0.083\,\mathrm{s^{-1}}$), the shear strain progresses to the maximum 100% from the initial 0% in a relatively short time (e.g. 12 s). The external magnetic field can only drive the microstructure's evolution to some extent, and the shear-induced deformation mainly dominates the microstructure's evolution. The enhancement of the macroscopic shear stress mainly results from the contribution of the magneto-enhanced initial yield shear stress and the contribution of the shear rate-enhanced shear stress. With the increasing shear rate, the contribution of the shear rate-enhanced shear stress sensitively enlarges significantly, while the contribution of the magneto-enhanced shear stress changes little with the increasing shear rate as the magneto-enhanced shear stress mostly depends on the external magnetic strength. This results in a decreased relative magneto-induced effect with the increased shear rate.

From section 3, one can see that the MRP's shape and the internal particle-formed microstructure can be dramatically tuned by the external magnetic field, inducing the axial (normal) stress along the field's direction. Thus, it is attractive to study the magneto-induced normal stress in the cyclically shearing process of the MRP. Corresponding to figure 8, the evolution of the magneto-induced normal stress with the cyclically shearing process under a different external magnetic field is shown in figure 10. In the absence of an external magnetic field, the normal stress σ_n is nearly zero and changes little in the shearing process. When the external magnetic field is $\mathrm{H = 95.6\,kA\,m^{-1}}$, the initial magneto-induced normal stress is about 2.5 kPa. In the beginning range (i.e. the shear strain increases from the initial 0% to about 5%), the normal stress slightly increases. This may result from the contribution of the chain-like microstructures' interaction. With the shear strain continuing to enlarge, the normal stress gradually goes down. This effect results from the complex coupled effects of the reduction of the normal stress component (as the preformed microstructure inclines), the rupture of the chain-like microstructure, etc. After the chain-like microstructure is lengthened, the interparticle gap in the chain-like microstructure

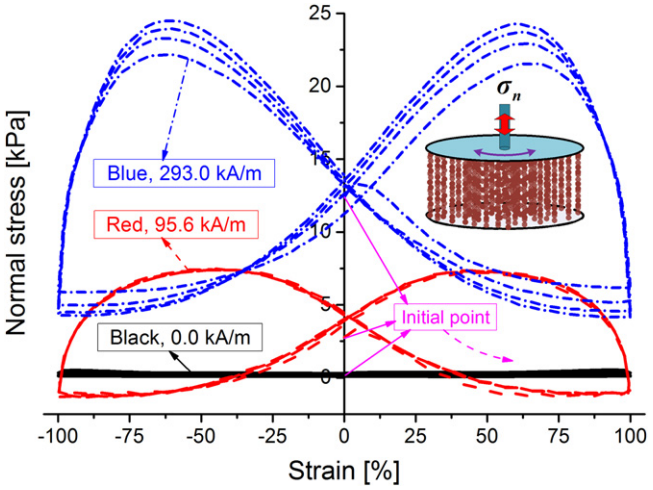

Figure 10. The magneto-induced normal stress's variation in the MRP-60 with the cyclically varying shear strain under a different external magnetic field. The purple dash arrow denotes the initial varying direction of the normal stress. The inset shows the initial preformed microstructure in the MRP.

appears. The gap induces a negative contribution to the normal stress since the attracting interaction between the upper particle and the lower particle still exists. When the shear strain inversely approaches 0% after it reaches the maximum, the internal particle-formed microstructure begins to reconstruct and contribute to the normal stress again. However, the reconstructed microstructure will rupture again after the reconstructed structure is squeezed to a certain extent. This effect results in the appearance of the peaks of magneto-induced normal stress. When $\mathrm{H = 293.0\,kA\,m^{-1}}$ (i.e. the magnetic strength is enough to timely tune the internal microstructure of the MRP), the initial magneto-induced normal stress enhances greatly to 12.4 kPa, and the normal stress changes in a large range from 4.3 to 24.5 kPa. The reconstruction and the rupture of the internal particle-formed microstructure progress simultaneously, and their contributions to the macroscopic normal stress are contrary. When the effect of the rupture (including the microstructure's incline) is larger than that of the reconstruction, the normal stress will drop. Contrarily, the normal stress will rise when the effect of the reconstruction is larger than that of the rupture. It can clearly be seen that the magneto-induced normal stress can be tuned in a large range and will enhance significantly after several cycles. To the best of our knowledge, this enhancement may result from the contribution of separated particles and short chains that assemble into main chain-like or column-like structures. This actuating mode in the normal or axial direction using transverse torsional shear is a new actuating mode in magnetorheology.

5. Conclusions

In this work, the magneto-induced large deformation effect of the MRP is reported, and the magneto-damping performance of the MRP under a quasi-statically shearing condition is

studied. From the study on the magneto-induced large deformation of an MRP, one can determine that the external magnetic field can tune the deformation of the MRP, and it is shown that the magneto-induced stress in the MRP drives the deformation. For the polyurethane-based MRP composited with 70 wt % CIP, the magneto-induced axial stress in the MRP can be tuned in a large range from 0.0 kPa to 55.4 kPa by a 662.6 kA m^{-1} magnetic field. From the study on the mechanical behavior of the MRP under a quasi-statically shearing condition, it is demonstrated that an MRP possesses a magneto-sensitive plastic malleability, and the magneto-mechanical behavior of an MRP can be described using a modified Bingham fluid model. The damping performance of the MRP has a significant positive correlation with the external magnetic strength, the shear rate, the CIP content and the amplitude of the shear strain. For an MRP with 60 wt % CIP, the relative magneto-enhanced damping effect can reach as high as 716.2% under an external 293.0 kA m^{-1}magnetic field. Moreover, one can recognize that the magneto-induced normal stress can be tuned in a large range from 4.3 kPa to 24.5 kPa along with the cyclically shearing process, and the normal stress will be significantly enhanced after several shearing cycles. This work demonstrates that MRPs have great potential for use in prospective dampers and actuators.

Acknowledgments

The financial support of the National Natural Science Foundation of China (Grant Nos. 11125210, 11102202), the National Basic Research Program of China (973 Program, grant no. 2012CB937500) and the Anhui Provincial Natural Science Foundation of China (1408085QA17) are gratefully acknowledged.

References

[1] Xu Y G, Gong X L, Xuan S H, Zhang W and Fan Y C 2011 A high-performance magnetorheological material: preparation characterization and magnetic-mechanic coupling properties *Soft Matter* **7** 5246–54

[2] de Vicente J, Klingenberg D J and Hidalgo-Alvarez R 2011 Magnetorheological fluids: a review *Soft Matter* **7** 3701–10

[3] Park B J, Fang F F and Choi H J 2010 Magnetorheology: materials and application *Soft Matter* **6** 5246–53

[4] Bica I, Liu Y D and Choi H J 2013 Physical characteristics of magnetorheological suspensions and their applications *J. Ind. Eng. Chem.* **19** 394–406

[5] Rodríguez-Arco L, Kuzhir P, López-López M T, Bossis G and Durán J D G 2013 Instabilities of a pressure-driven flow of magnetorheological fluids *J. Rheol.* **57** 1121–46

[6] Sedlacik M, Pavlinek V, Vyroubal R, Peer P and Filip P 2013 A dimorphic magnetorheological fluid with improved oxidation and chemical stability under oscillatory shear *Smart Mater. Struct.* **22** 035011

[7] Li W H, Zhang X Z and Du H 2013 Magnetorheological elastomers and their applications ed P M Visakh, S Thomas, A K Chandra and A P Mathew *Advances in Elastomers I: Blends and Interpenetrating Networks* pp 357–74(Berlin, Germany: Springer)

[8] Danas K, Kankanala S V and Triantafyllidis N 2012 Experimental and modeling of iron-particle-filled magnetorheological elastomers *J. Mech. Phys. Solids* **60** 120–38

[9] Li W H and Zhang X Z 2010 A study of the magnetorheological effect of bimodal particle based magnetorheological elastomers *Smart Mater. Struct.* **19** 035002

[10] Wang D H and Liao W H 2011 Magnetorheological fluid dampers: a review of parametric modelling *Smart Mater. Struct.* **20** 023001

[11] Liao W H and Wang D H 2003 Semiactive vibration control of train suspension systems via magnetorheological dampers *J. Intell. Mater. Syst. Struct.* **14** 161–72

[12] Zong L H, Gong X L, Xuan S H and Guo C Y 2013 Semi-active H∞ control of high-speed railway vehicle suspension with magnetorheological dampers *Veh. Syst. Dyn.* **32** 479–97

[13] Hoang N, Zhang N, Li W H and Du H 2013 Development of a torsional dynamic absorber using a magnetorheological elastomer for vibration reduction of a powertrain test rig *J. Intell. Mater. Syst. Struct.* **24** 2036–44

[14] Liao G J, Gong X L, Kang C J and Xuan S H 2011 The design of an active-adaptive tuned vibration absorber based on magnetorheological elastomer and its vibration attenuation performance *Smart Mater. Struct.* **20** 075015

[15] Yang J, Du H P, Li W H, Li Y C, Li J C, Sun S S and Deng H X 2013 Experimental study and modeling of a novel magnetorheological elastomer isolator *Smart Mater. Struct.* **22** 117001

[16] Behrooz M, Wang X J and Gordaninejad F 2014 Modeling of a new semi-active/passive magnetorheological elastomer isolator *Smart Mater. Struct.* **23** 045013

[17] Bica I 2011 Magnetoresistor with magnetorheological elastomers *J. Ind. Eng. Chem.* **17** 83–9

[18] Ausanio G, Iannotti V, Ricciardi E, Luca L and Lanotte L 2014 Magneto-piezoresistance in magnetorheological elastomers for magnetic induction gradient or position sensors *Sens. Actuators* A **205** 235–9

[19] Kashima S, Miyasaka F and Hirata K 2012 Novel soft actuator using magnetorheological elastomer *IEEE Trans. Magn.* **48** 1649–52

[20] Xu Y G, Gong X L, Xuan S H, Li X F, Qin L J and Jiang W Q 2012 Creep and recovery behaviors of magnetorheological plastomer and its magnetic-dependent properties *Soft Matter* **8** 8483–92

[21] Gong X L, Xu Y G, Xuan S H, Guo C Y, Zong L H and Jiang W Q 2012 The investigation on the nonlinearity of plasticine-like magnetorheological material under oscillatory shear rheometry *J. Rheol.* **56** 1375–91

[22] Sutton M 2008 *Digital Image Correlation for Shape and Deformation Measurements, in Springer Handbook of Experimental Solid Mechanics* ed J Sharpe and N William (US: Springer) pp 565–600

[23] Gong X L, Guo C Y, Xuan S H, Liu T X, Zong L H and Peng C 2012 Oscillatory normal forces of magnetorheological fluids *Soft Matter* **8** 5256–61

[24] Guo C Y, Gong X L, Xuan S H, Zong L H and Peng C 2012 Normal forces of magnetorheological fluids under oscillatory shear *J. Magn. Magn. Mater.* **324** 1218–24

[25] An H N, Picken S J and Mendes E 2012 Direct observation of particle rearrangement during cyclic stress hardening of magnetorheological gels *Soft Matter* **8** 11995–2001

[26] An H N, Sun B, Picken S J and Mendes E 2012 Long time response of soft magnetorheological gels *J. Phys. Chem.* B **116** 4702–11

[27] Ju B X, Yu M, Fu J, Zheng X and Liu S Z 2013 Magnetic field-dependent normal force of magnetorheological gel *Ind. Eng. Chem. Res.* **52** 11583–11589

[28] Liu T X, Gong X L, Xu Y G, Xuan S H and Jiang W Q 2013 Simulation of magneto-induced rearrangeable microstructures of magnetorheological plastomers *Soft Matter* **9** 10069–80

[29] Liu T X, Xu Y G, Gong X L, Pang H M and Xuan S H 2013 Magneto-induced normal stress of magnetorheological plastomer *AIP Adv.* **3** 082122

[30] Melenev P V, Raikher Y L and Rusakov V V 2010 Plasticity of soft magnetic elastomers *Polymer Science Ser.* A **52** 430–5

[31] Melenev P V, Raikher Y L, Stepanov G, Rusakov V V and Polygalova L 2011 Modeling of the field-induced plasticity of soft magnetic elastomers *J. Intell. Mater. Syst. Struct.* **22** 531–8

[32] Stolbov O V, Raikher Y L and Balasoiu M 2011 Modelling of magnetodipolar striction in soft magnetic elastomers *Soft Matter* **7** 8484–7